J|A|C|S
ARTICLES
Published on Web 09/13/2002

Functional Analogues of the Dioxygen Reduction Site in Cytochrome Oxidase: Mechanistic Aspects and Possible Effects of Cu_B

Roman Boulatov, James P. Collman,* Irina M. Shiryaeva, and Christopher J. Sunderland

Contribution from the Department of Chemistry, Stanford University, Stanford, California 94309

Received March 12, 2002

Abstract: Catalytic reduction of O_2 and H_2O_2 by new synthetic analogues of the heme/Cu site in cytochrome *c* and ubiquinol oxidases has been studied in aqueous buffers. Among the synthetic porphyrins yet reported, those employed in this study most faithfully mimic the immediate coordination environment of the Fe/Cu core. Under physiologically relevant conditions, these biomimetic catalysts reproduce key aspects of the O_2 and H_2O_2 chemistry of the enzyme. When deposited on an electrode surface, they catalyze the selective reduction of O_2 to H_2O at potentials comparable to the midpoint potential of cytochrome *c*. The pH dependence of the half-wave potentials and other data are consistent with O−O bond activation at these centers proceeding via a slow generation of a formally ferric-hydroperoxo intermediate, followed by its rapid reduction to the level of water. This kinetics is analogous to that proposed for the O−O reduction step at the heme/Cu site. It minimizes the steady-state concentration of the catalytic intermediate whose decomposition would release free H_2O_2. The maximum catalytic rate constants of O_2 reduction by the ferrous catalyst and of H_2O_2 reduction by both ferric and ferrous catalysts are comparable to those reported for cytochrome oxidase. The oxidized catalyst also displays catalase activity. Comparison of the catalytic properties of the biomimetic complexes in the FeCu and Cu-free forms indicates that, in the regime of rapid electron flux, Cu does not significantly affect the turnover frequency or the stability of the catalysts, but it suppresses superoxide-releasing autoxidation of an O_2−catalyst adduct. The distal Cu also accelerates O_2 binding and minimizes O−O bond homolysis in the reduction of H_2O_2.

Introduction

The exergonic four-electron (*4e*) reduction of O_2 to the redox level of water is of great biological and technological (e.g., fuel cells) significance. In an aerobic organism, O_2 is utilized in a variety of biochemical transformations that are fundamental to most stages of the cellular life cycle. Over 95% of consumed dioxygen is used in respiration,[1] whereby O_2 is reduced to H_2O by multiunit membrane enzymes in the superfamily of heme/Cu terminal oxidases (e.g., cytochrome *c* oxidase[2−5] and ubiquinol oxidase[6]). Unlike other heme enzymes of oxygen metabolism (e.g., oxygenases, peroxidases,[7−12] and catalases[13]), the catalytic site of terminal oxidases is bimetallic (Figure 1).[14] In addition, various terminal oxidases have one, two, or three electron-transfer sites. In cytochrome oxidase, two redox cofactors (Cu_A and heme a) mediate electron transfer between cytochrome *c* and the heme/Cu site. In catalytically active forms of cytochrome oxidase, the heme/Cu site is fully reduced (Fe^{II}/Cu^{I}), whereas the electron-transfer sites can be fully oxidized (Cu_A^{II}, Fe_a^{III}: mixed-valence enzyme), partially oxidized, or reduced (Cu_A^{I}, Fe_a^{II}: fully reduced enzyme). Although the population of these redox states in vivo is unknown, Wikström recently argued that, even in normoxic tissues, a large fraction of the enzyme may be fully reduced.[15]

Even though its catalytic site is bimetallic, the reduction of O_2 by cytochrome oxidase (Figure 2) appears to proceed via intermediates that are similar, with respect to the binding modes of O_2 and its derivatives, to those observed in monometallic heme enzymes. Oxyheme (compound A) and various oxoferryl intermediates (compounds P_R, P_M and F) have been observed

(1) Babcock, G. T. *Proc. Natl. Acad. Sci. U.S.A.* **1999**, *96*, 12971.
(2) Michel, H.; Behr, J.; Harrenga, A.; Kannt, A. *Annu. Rev. Biophys. Biomol. Struct.* **1998**, *27*, 329.
(3) Pereira, M. M.; Santana, M.; Teixeira, M. *Biochim. Biophys. Acta* **2001**, *1505*, 185.
(4) Zaslavsky, D.; Gennis, R. B. *Biochim. Biophys. Acta* **2000**, *1458*, 164.
(5) Ferguson-Miller, S.; Babcock, G. T. *Chem. Rev.* **1996**, *96*, 2889.
(6) Abramson, J.; Riistama, S.; Larsson, G.; Jasaitis, A.; Svensson-Ek, M.; Laakkonen, L.; Puustinen, A.; Iwata, S.; Wikström, M. *Nat. Struct. Biol.* **2000**, *7*, 910.
(7) Sono, M.; Roach, M. P.; Coulter, E. D.; Dawson, J. H. *Chem. Rev.* **1996**, *96*, 2841.
(8) Poulos, T. L. In *The Porphyrin Handbook*; Kadish, K. M., Smith, K. M., Guilard, R., Eds.; Academic Press: San Diego, CA, 2000; Vol. 4, pp 189−218.
(9) Traylor, T. G.; Traylor, P. S. In *Active Oxygen in Biochemistry*; Valentine, J. S., Foote, C. S., Greenberg, A., Liebman, J. F., Eds.; Chapman and Hall: New York, 1995; Vol. 3, pp 84−187.
(10) Loew, G. H.; Harris, D. L. *Chem. Rev.* **2000**, *100*, 407.
(11) Veitch, N. C.; Smith, A. T. *Adv. Inorg. Chem.* **2001**, *51*, 107.
(12) de Montellano, P. R. O. *Cytochrome P450*, 2nd ed.; Plenum: New York, 1995.
(13) Nicholls, P.; Fita, I.; Loewen, P. C. *Adv. Inorg. Chem.* **2001**, *51*, 51.
(14) Yoshikawa, S.; Shinzawa-Itoh, K.; Nakashima, R.; Yaono, R.; Yamashita, E.; Inoue, N.; Yao, M.; Fei, M. J.; Libeu, C. P.; Mizushima, T.; Yamaguchi, H.; Tomizaki, T.; Tsukihara, T. *Science* **1998**, *280*, 1723.
(15) Morgan, J. E.; Verkhovsky, M. I.; Palmer, G.; Wikström, M. *Biochemistry* **2001**, *40*, 6882.

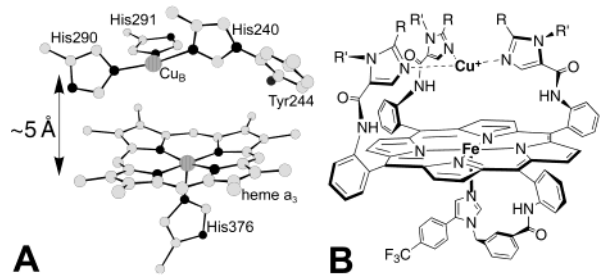

Figure 1. (A) Heme a_3/Cu_B site of bovine cytochrome oxidase.[14] The C atoms are light gray, the N and O atoms are black, and the Fe and Cu ions are dark gray. (B) General chemical structure of the catalysts (in the reduced $Fe^{II}Cu^{I}$ form); any exogenous ligands and/or counterions are omitted. In the FeZn derivative, Zn substitutes for Cu. For synthesis and spectroscopic characterization, see ref 23. Three series of catalysts (R = H, R′ = CH_3; R = $(CH_2)_2CH_3$, R′ = H; R = $(CH_2)_2CH_3$, R′ = CH_3) manifest similar electrocatalytic behavior.

spectroscopically,[1−5,16] whereas the intermediacy of a ferric-hydroperoxo species is postulated on the basis of DFT calculations.[17] The distribution of oxidizing equivalents among various redox-active enzymatic sites during turnover depends on the initial redox state of cytochrome oxidase. The reaction of O_2 with the mixed-valence enzyme generates an oxoferryl-tyrosine radical intermediate (compound P_M),[16a] which is stable until additional reducing equivalents enter the enzyme. In contrast, the reduction of O_2 by fully reduced cytochrome oxidase is coupled to the oxidation of Cu_B, Fe_{a3}, and Fe_a and, hence, does not generate organic radicals (Figure 2).[15] Importantly, the formation of catalytic intermediates wherein the O_2-derived moiety is bound to both metals (e.g., $Im_3Cu_B-O-O-Fe$) is not supported by spectroscopic[16b] or computational studies.[17] In contrast to O_2, H_2O_2 is reduced to the level of water by any of the five redox states of cytochrome oxidase.[4]

While the reduction of O_2 under steady-state conditions is generally believed to be coupled to the oxidation of Cu_B^I (Figure 2), it remains uncertain if Cu_B serves mainly as an electron storage site in the heme proximity or provides a unique reaction pathway that is not accessible for the O−O bond activation by the heme alone.[4] Another important issue of whether a nonredox stereoelectronic influence of the closely positioned Cu_B modifies the heme reactivity is virtually unexplored. Cu_B-free variants of terminal oxidases, obtained by mutation of Cu-ligating histidine(s), have been little studied.[18−21] These mutants are catalytically inactive even though they appear to retain the interheme electron-transfer rate of wild-type analogues.[20] In addition, lower on-rates of CO and both higher and lower CO binding constants have also been reported for Cu_B-free terminal oxidases.[18,19]

Biomimetic studies can be a fruitful strategy to address questions that cannot be probed by working with the enzyme itself. The heme/Cu site of terminal oxidases has long been a target for biomimetic studies.[22] Yet, despite an enormous amount of work, the potential of the biomimetic approach to contribute to understanding the reactivity of terminal oxidases remains woefully underrealized. The reactivities of synthetic heme/Cu analogues, especially under catalytic and physiologically relevant conditions, have been little studied. Model systems that faithfully reproduce the stereoelectronic environment of the heme/Cu site have been difficult to design and synthesize. As a result, the reactivities of most synthetic heme/Cu analogues studied to date differ notably from that observed with the enzyme. Consequently, the conclusions that have been drawn for such studies have limited enzymatic relevance.

We have recently reported[23] a new series of synthetic heme/Cu analogues, which, among any complexes yet synthesized, most faithfully mimic the coordination environment of the Fe/Cu core. Herein, we report the catalytic behaviors of these complexes in the electrochemical reductions of O_2 and H_2O_2 in neutral aqueous buffers under physiologically relevant conditions and rapid electron flux. First, we establish that these complexes quantitatively reproduce several key aspects of the reactivity of cytochrome oxidase. Second, we compare the catalytic behaviors of these biomimetic catalysts in the FeCu and Cu-free forms. On the basis of these data and the structural and functional fidelity of our complexes as heme/Cu analogues, we propose how Cu_B may affect the reactivity of the heme in cytochrome oxidase.

Results

Our water-insoluble catalysts were studied as films deposited on an electrode surface (usually edge-plane graphite, EPG) in contact with an aqueous electrolyte. In most experiments, the amount of the catalyst per *geometric* surface area of the electrode (geometric surface coverage, Γ_t) was ~2.5 nmol/cm^2, which corresponds to a few effective monolayers.[24,25]

Electrochemistry in the Absence of Substrates. In the absence of a substrate, both the Fe-only and FeCu catalysts exhibit single symmetric oxidation and reduction peaks centered around ~100 mV (Figure 3). Integration of these peaks above an interpolated baseline yields a geometric surface coverage of ~2.4 nmol/cm^2, on the basis of single ($Fe^{III/II}$) and double ($Fe^{III}Cu^{II}/Fe^{II}Cu^{I}$) electron redox processes for Fe-only and FeCu catalysts, respectively. The data indicate that surface-confined FeCu catalysts in contact with an aqueous electrolyte retain Cu and that the $Cu^{II/I}$ redox potential is close to that of the Fe. In cytochrome oxidase, the $Fe_{a3}^{III/II}$ and $Cu_B^{II/I}$ potentials are also similar but are higher than those of our catalysts.

Fast in-film charge transfer is evidenced by the direct proportionality of the peak current and the scan rate.[26] The nonzero scan-rate-independent peak separation (ΔE_p) and the peak widths at half-height (fwhh = 180−190 mV) in excess of 91 mV are not uncommon for redox films.[35,36] In our systems,

(16) (a) Proshlyakov, D. A.; Pressler, M. A.; DeMaso, C.; Leykam, J. F.; DeWitt, D. L.; Babcock, G. T. *Science* **2000**, *290*, 1588. (b) Fabian, M.; Wong, W. W.; Gennis, R. B.; Palmer, G. *Proc. Natl. Acad. Sci. U.S.A.* **1999**, *96*, 13114.
(17) Blomberg, M. R. A.; Siegbahn, P. E. M.; Babcock, G. T.; Wikström, M. *J. Am. Chem. Soc.* **2000**, *122*, 12848.
(18) Calhoun, M. W.; Hill, J. J.; Lemieux, L. J.; Ingledew, W. J.; Alben, J. O.; Gennis, R. B. *Biochemistry* **1993**, *32*, 11524.
(19) Mogi, T.; Hirano, T.; Nakamura, H.; Anraku, Y.; Orii, Y. *FEBS Lett.* **1995**, *370*, 259.
(20) Brown, S.; Rumbley, J. N.; Moody, A. J.; Thomas, J. W.; Gennis, R. B.; Rich, P. R. *Biochim. Biophys. Acta* **1994**, *1183*, 521.
(21) Lemon, D. D.; Calhoun, M. W.; Gennis, R. B.; Woodruff, W. H. *Biochemistry* **1993**, *32*, 11953.
(22) Collman, J. P.; Boulatov, R.; Sunderland, C. J. In *The Porphyrin Handbook*; Kadish, K. M., Smith, K. M., Guilard, R., Eds.; Academic Press: San Diego, 2003; Vol. 11, in press.
(23) Collman, J. P.; Sunderland, C. J.; Boulatov, R. *Inorg. Chem.* **2002**, *41*, 2282.
(24) When the packing density of the catalyst molecules on the surface are similar to that in the solid state,[25a] a monolayer on a smooth surface corresponds to $\Gamma_t \approx 0.2$ nmol/cm^2. An EPG surface freshly polished with 600 grit SiC paper has a roughness factor of ~3−5.[25b]
(25) (a) Collman, J. P.; Berg, K.; Sunderland, C. J.; Vance, M. A.; Solomon, E. I. *Inorg. Chem.* **2002**, in press. (b) McCreery, R. L. *Electroanal. Chem.* **1990**, *17*, 221.
(26) See the Supplementary information for the relevant figures.

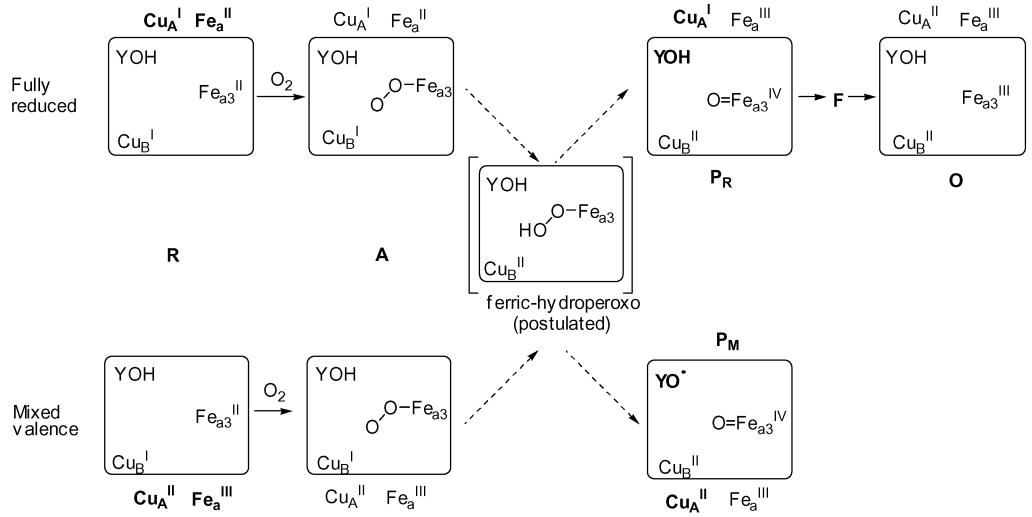

Figure 2. Mechanism of O_2 reduction by the fully reduced and mixed-valence forms of cytochrome oxidase. The rectangle represents the heme a_3/Cu_B site; YOH is the tyrosine residue. The differences in the locations of oxidizing equivalents in the starting forms and compounds P are highlighted in bold. Distribution of the reducing equivalent between Cu_A and Fe_a differentiates compounds P_R and F.[15]

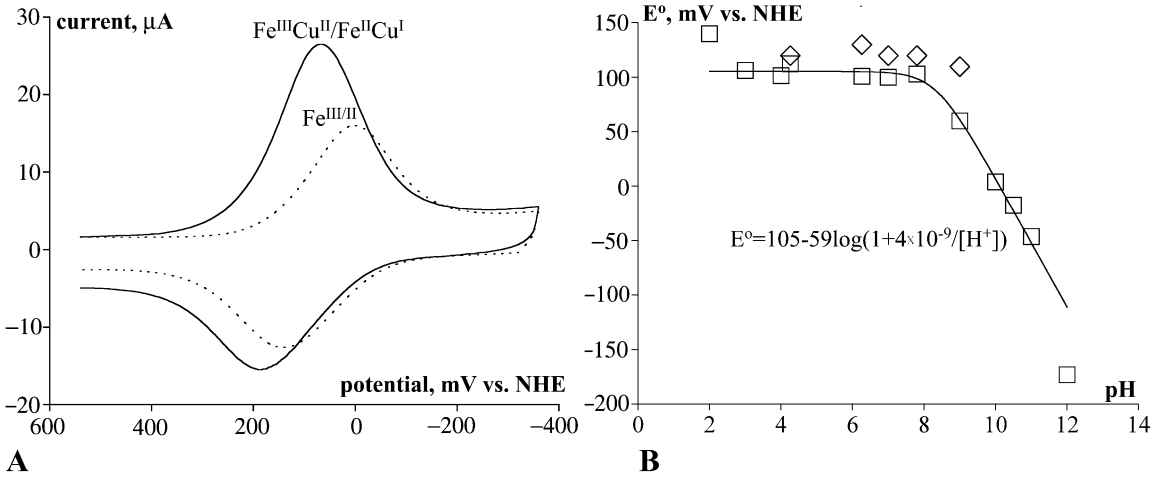

Figure 3. (A) Typical cyclic voltammograms of the FeCu (solid line) and Fe-only (dotted line) catalysts in anaerobic pH 7 buffer; scan rate 50 mV/s. (B) pH dependence of the $Fe^{III}Cu^{II}/Fe^{II}Cu^{I}$ (◇) and $Fe^{III/II}$ (□) potentials ($E°$). The FeCu complex does not retain Cu below pH 4. The solid line: least-squares fit of the Fe-only data to the equation shown. The deviations at pH = 2 and 12 may reflect ligand-based protolytic processes affecting $E°$.

they appear to be due to slow phase transitions within partially reduced catalytic films and interactions among redox sites, respectively.[27] The fwhh and ΔE_p are largely independent of the amount of deposited catalyst or the electrode material.

The pH dependence of the $Fe^{III/II}$ potential of the Fe-only catalysts (Figure 3B) indicates that the dominant ligation state of the ferric complex is six-coordinate $pFe^{III}(OH_2)^+$ at pH < 9.[28−31] From differences in the apparent affinities of CN^- to the ferric Fe-only catalyst measured under noncatalytic and catalytic conditions,[32] an ∼1000:1 fractionation between six-coordinate $pFe^{III}(OH_2)^+$ and five-coordinate pFe^+ is estimated at pH 7. A similar method yields a ratio of ∼150:1 for the fractionation between six- and five-coordinate *ferrous* forms ($pFe^{II}(OH_2)$ vs pFe^{II}). The nearly identical $Fe^{III/II}$ potentials in the Fe-only and FeCu catalysts (Figure 3B) suggest a similar ligation of Fe. We have previously shown that both Cu^I and Cu^{II} coordinated in the trisimidazole superstructure bind various ligands at the fourth coordination site.[23] Because the nature of the buffer does not affect the $Cu^{I/II}$ potential in the complex on the electrode surface, this site is likely occupied by a water-derived ligand. From an electrostatic consideration, it seems likely that one OH^- is present in the oxidized catalyst to compensate the +3 charge of the $Fe^{III}Cu^{II}$ core. Therefore, the most plausible ligation of the $Fe^{III}Cu^{II}$ core is $FeOH_2^+/CuOH^+$ at $4 \le pH \le 9$ (the FeCu catalyst does not retain Cu below pH 4), which is identical to that in compound O (Figure 2).[33] The

(27) Shiryaeva, I. M.; Collman, J. P.; Boulatov, R.; Sunderland, C. J. *Anal. Chem.* **2002**, submitted.
(28) The pK_a value of this water molecule (8.4(1)) is higher than those reported for bisaqua-ligated ferric porphyrins (e.g., 7.25[29] or 6.55[31] in tetrakis(2,6-dimethyl-3-sulfonatophenyl)porphyrinatoiron(III); 5.1−5.5 in various tetrakis(*N*-methyl-*n*-pyridyl)porphyrinatoiron(III), $n = 2-4$[30]), probably reflecting the additional stabilization of the positive charge by the more σ-basic proximal imidazole.
(29) Kaaret, T. W.; Zhang, G.-H.; Bruice, T. C. *J. Am. Chem. Soc.* **1991**, *113*, 4652.
(30) Su, Y. O.; Kuwana, T.; Chen, S. M. *J. Electroanal. Chem.* **1990**, *288*, 177.
(31) Zipplies, M. F.; Lee, W. A.; Bruice, T. C. *J. Am. Chem. Soc.* **1986**, *108*, 4433.
(32) Boulatov, R.; Collman, J. P.; Shiryaeva, I. M.; Sunderland, C. J. *Angew. Chem., Int. Ed.* **2002**, in press.
(33) Yoshikawa, S.; Mochizuki, M.; Zhao, X.-J.; Caughey, W. S. *J. Biol. Chem.* **1995**, *270*, 4270.
(34) He, B.; Sinclair, R.; Copeland, B. R.; Makino, R.; Powers, L. S.; Yanazaki, I. *Biochemistry* **1996**, *35*, 2413.
(35) See for example chapter 14 in ref 36.
(36) Bard, A. J.; Faulkner, L. R. *Electrochemical Methods*; Wiley: New York, 2001.

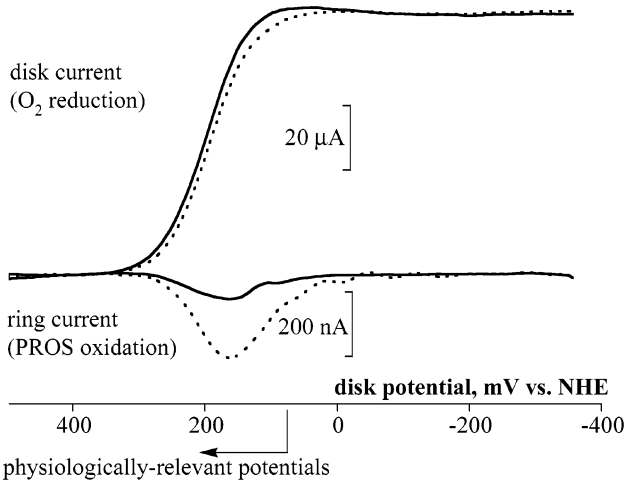

Figure 4. Typical LSVs of electrocatalytic O_2 reduction by the FeCu (solid line) and Fe-only (dotted line) catalysts in an air-saturated pH 7 buffer at 200 rpm. Scan rate 10 mV/s; ring collection efficiency 15%. Note the different scales for i_r and i_{cat}. The LSV generated by the FeZn catalyst is insignificantly different from that of the Fe-only analogue. The midpoint potentials of cytochrome *c* (~250 mV) and ubiquinol (≥50 mV), which are the physiological electron donors to cytochrome and (functionally related) ubiquinol oxidases, define the "physiologically relevant potential range".

+2 charge of the oxidized catalyst may be stabilized by partial charge delocalization over both distal and proximal imidazoles, as proposed for cytochrome oxidase.

At highly oxidizing potentials, the catalysts manifest an additional one-electron redox process, assigned to the $Fe^{IV/III}$ couple.[26] The average of the anodic and cathodic peak potentials at pH 7 (0.95 V) is similar to the potential of the $pFe(OH_2)^+/pFe^{IV}{=}O$ couple in hemoproteins (e.g., compound II of horseradish peroxidase and myoglobin)[34] and in model compounds (0.9−0.98 V).[29] The substitution of Fe by Zn eliminates this high-potential process, which rules out the possibility that it belongs to a ligand-based couple.

O_2 Reduction at pH 7. Typical linear sweep voltammograms (LSVs) on a Pt-ring/EPG-disk rotating electrode (RRDE)[36] in an air-saturated pH 7 buffer are shown in Figure 4. Catalysis commences at ~300 mV and, as the disk potential is made increasingly reducing, the reaction accelerates until its rate becomes potential-independent (the plateau region), at ~100 mV. At the potential-dependent part of the wave, one or more redox steps are sufficiently unfavorable to limit the turnover frequency, whereas, at the plateau, the catalytic rate is determined solely by the rate(s) of nonredox step(s).

The ring current (i_r, lower curves, Figure 4) is generated by oxidation at the Pt ring of a fraction of partially reduced oxygen species (PROS, H_2O_2, and/or O_2^-) released by the catalytic film into the electrolyte. The selectivity of the catalysts toward the *4e* O_2 reduction at any electrochemical potential is quantified by the ratio of the ring and catalytic (disk) currents, i_r/i_{cat}, corrected for the ring collection efficiency.[37] Because Pt is easily deactivated toward H_2O_2 oxidation, the collection efficiency of H_2O_2 (N_{per}) is always lower than the theoretical one or the collection efficiency measured with simple redox couples (i.e., $Fe(CN)_6^{3-/4-}$). Failure to account for this effect results in significantly overestimated catalytic selectivities.[22] We undertook several precautions (see the Experimental Section) to maximize N_{per} and to know its precise value in every electrocatalytic experiment. Hence, the low i_r/i_{cat} ratios observed in this work are not artifacts but reflect the high selectivity of our catalytic films toward *4e* O_2 reduction. The potential-dependent i_r is fully consistent with the nature of the primary PROS (O_2^-)[38] and the catalytic mechanism, as discussed below.

The LSVs in Figure 4 represent the steady-state behavior of the catalytic film. This is evident from the independence of the half-wave potentials and the i_r/i_{cat} ratios on the scan rate (1−50 mV/s) or its direction and the amount of the catalyst (0.1−25 nmol/cm^2) at a fixed electrode rotation frequency. The i_r/i_{cat} ratio is also invariant to the O_2 tension (0.1−1 bar; $\Gamma_t \geq 0.1$ nmol/cm^2).

Linear Koutecky−Levich (KL) plots[36] (i_{cat}^{-1} vs $\omega^{-1/2}$, where ω is the electrode rotation frequency) confirm the essentially *4e* stoichiometry of the O_2 reduction observed in the RRDE experiments (Figure 5). The inverse dependence of the slopes and the intercepts of these graphs on an O_2 tension[26] establishes that the KL equation is an adequate description of the catalytic kinetics in our systems. The slopes are equal to that measured for O_2 reduction on thoroughly cleaned Pt (the *4e* standard) and are half the slope for O_2 reduction on EPG (the *2e* standard). At a given O_2 tension, the slopes are independent of the amount of the deposited catalyst down to submonolayer surface coverages. Kinetic currents, i_k (the inverse intercepts of KL graphs), are proportional to the catalyst surface coverage, Γ_t (up to 2.5 nmol/cm^2).[26] The proportionality constant corresponds to the maximum apparent rate constants of O_2 reduction by the FeCu and the Fe-only catalysts (1.2×10^5 and 5.1×10^4 $M^{-1}s^{-1}$, respectively).

In contrast to the case of other metalloporphyrins that catalyze *4e* O_2 reduction when adsorbed on edge-plane graphite but are largely *2e* catalysts on other surfaces,[40] our catalysts retain the *4e* activity when deposited on a basal plane, glassy carbon, or Au electrodes.[26]

Nature of the Primary PROS in O_2 Reduction at Physiological Potentials. In O_2 reduction at physiologically relevant potentials, the FeCu and Cu-free catalysts differ mainly by the amount of PROS released into the electrolyte, with the FeCu complex being a more selective catalyst, as evidenced by its smaller i_r/i_{cat} ratio (Figure 4). We considered a possibility that the lower PROS release from the FeCu film originates mainly from PROS sinks unique to this film due to its higher charge density or multiple Cu sites. To probe this, we changed the charge density of, and Cu concentration in, the FeCu and Fe-only films by diluting them with structurally analogous but inert Zn-only and ZnCu (Zn substitutes for Fe) derivatives. Such films displayed i_r/i_{cat} ratios insignificantly different from those of

(37) The formula relating the i_r/i_d ratio and the fraction of the *4e* pathway depends on the composition of the PROS flux released by the catalyst. If the major primary PROS is H_2O_2, the fraction is expressed as $(1 - i_r/i_d)/(1 + i_r/i_d)$, whereas, in the case of O_2^-/HO_2, it is $(1 - i_r/i_d)/(1 + 3i_r/i_d)$.

(38) Collection efficiency-corrected i_r/i_{cat} ratios were calculated by dividing experimental i_r by N_{per} because the rapid dismutation of O_2^- into H_2O_2 and O_2 ($\geq 2 \times 10^5$ M^{-1} s^{-1} at pH 7) makes it unlikely that any catalyst-generated O_2^- reaches the ring. However, if some O_2^- is oxidized by the ring, dividing observed i_r by N_{per} overestimates the PROS flux (underestimate the catalytic selectivity) because the ring collection efficiency of O_2^- likely exceeds that for H_2O_2 (N_{per}). The latter is due to the *1e* oxidation of O_2^- being more favorable, both thermodynamically and kinetically, than the *2e*/$2H^+$ oxidation of H_2O_2.

(39) At a bulk O_2 concentration of 0.24 mM, taking the O_2 diffusion coefficient as 2.1×10^{-5} cm^2/s and solution viscosity as 0.01 s/cm.

(40) Hutchison, J. E.; Postlethwaite, T. A.; Chen, C.-h.; Hathcock, K. W.; Ingram, R. S.; Ou, W.; Linton, R. W.; Murray, R. W.; Tyvoll, D. A.; Chng, L. L.; Collman, J. P. *Langmuir* **1997**, *13*, 2143.

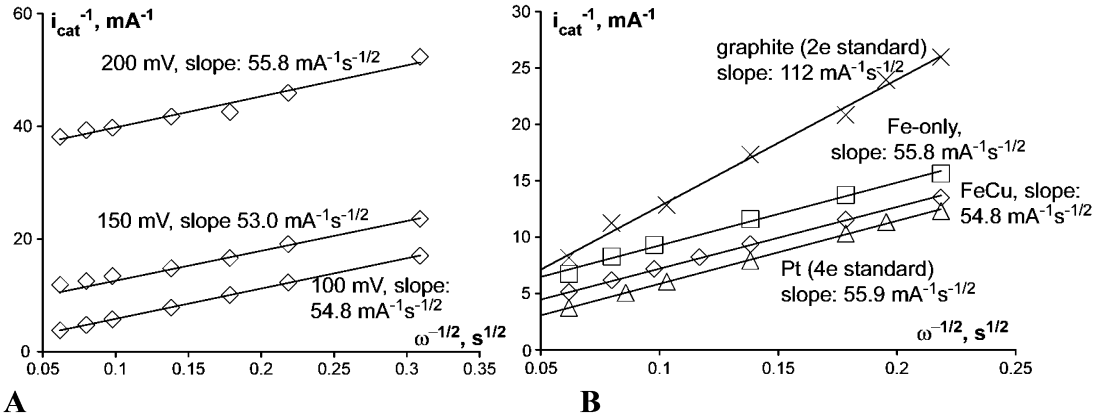

Figure 5. Koutecky−Levich plots for O_2 reduction currents in the air-saturated pH 7 buffer for the FeCu (◊) and Fe-only (□) catalysts (Γ_t = 0.25 nmol/cm^2) at the potential-dependent (A) and plateau (B) parts of the catalytic waves. For comparison, the limiting currents at the Pt (△, the *4e* standard) and bare EPG (×, the *2e* standard) electrodes are shown. The numbers indicate slopes of the least-squares fits (solid lines); the calculated slope for the *4e* O_2 reduction is 55 mA^{-1} s$^{-1/2}$.[39]

Table 1. Selectivities (i_r/i_{cat} Ratios) of the Fe-only and FeCu Films Containing O_2^-Antioxidants or Inert Structural Analogues, Relative to the Selectivities of the Respective Unmodified Films

			relative selectivities[b]	
entry	additive[a]	molar fraction	Fe-only catalyst	FeCu catalyst
1	Zn-only	0.5	1.1(1)	1.1(1)
2	ZnCu	0.5	0.8(2)	1.1(1)
3	BHT	0.2	1.3(1)	1.09(9)
4	trolox	0.2	1.5(2)	0.95(8)
5	MPG	0.2	1.8(2)	
6	MPG	0.5	2.2(2)	
7	2,3-NDA[c]	0.5	1.2(1)	1.1(2)
8	ebselen[c]	0.2−0.4	1.25(8)	1.2(1)
9	thiourea[c]	0.3	1.1(2)	1.1(1)

[a] Zn-only and ZnCu are the Fe-only and FeCu analogues, respectively, with Zn substituting for Fe (Figure 1B). See Figure 6 for chemical structures of the other additives. [b] The i_r/i_{cat} ratio of a modified film divided by the i_r/i_{cat} ratio of the film without an additive; both ratios were measured at the half-wave potentials; a value > 1 means that the modified film produces larger ring currents than the unmodified film at the same rate of O_2 reduction (constant i_{cat}). [c] Inert toward O_2^-/HO_2.

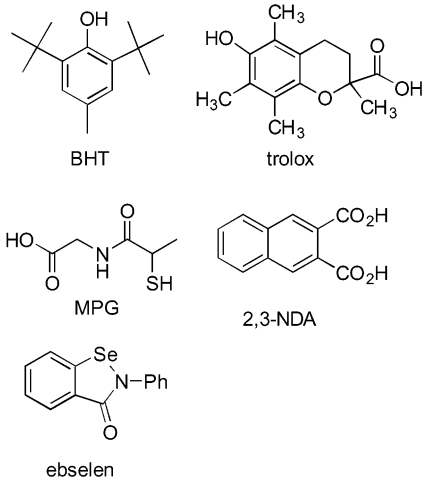

Figure 6. Superoxide reductants and inert analogues employed as film dilutants.

unmodified films (Table 1, entries 1 and 2). Hence, we conclude that the lower i_r/i_{cat} ratio of the FeCu film relative to that of the Cu-free analogues reflects the intrinsically higher selectivity of the FeCu molecule.

We find that O_2 reduction by the Cu-free, but not the FeCu, catalysts at 250−50 mV potentials is accompanied by the production of free O_2^- (or its conjugate acid, hydroperoxyl radical, HO_2, hereafter referred to as superoxide). Because the small ring currents generated by these catalysts may indicate either superoxide or H_2O_2 (or both) as the major primary PROS,[41] we examined how the ring currents are affected by selective superoxide antioxidants. The latter are organic compounds that reduce O_2^-/HO_2 to H_2O_2 at apparent second-order rate constants between 10^4−10^6 M^{-1} s^{-1} at pH 7.[42] The presence of redox-active organic compounds in the electrolyte is incompatible with using RRDE for PROS detection. Hence, the experiments were conducted with antioxidants incorporated into the catalytic film, which precluded the use of superoxide dismutase. We compared the i_r/i_{cat} ratios observed in O_2 reduction by mixed films of catalysts and BHT,[43] trolox,[44] or MPG[45] (Figure 6) with the i_r/i_{cat} ratios measured for unmodified films under the same conditions. In the absence of an antioxidant, most of the catalyst-generated O_2^- probably disproportionates biomolecularly into O_2 and H_2O_2 (with an apparent rate constant of 2×10^5 M^{-1} s^{-1} at pH 7) before diffusing into the electrolyte. In the simplest case, all O_2^- converts to 0.5 equiv of H_2O_2 and only H_2O_2 is oxidized at the ring. In the presence of an antioxidant, additional H_2O_2 is formed within the film as the catalyst-generated O_2^- is reduced by the antioxidant, resulting in a larger ring current. Therefore, a higher i_r/i_{cat} ratio of an antioxidant-modified catalytic film relative to an identical film without an antioxidant is an indication that the catalyst very likely releases O_2^-. The magnitude of this antioxidant-induced increase in the i_r/i_{cat} ratio is determined by the fraction of O_2^-/HO_2 in the catalyst-generated PROS flux and by the rate of superoxide reduction by the antioxidant relative to O_2^- diffusion out of the film and of all other O_2^--consuming secondary reactions (e.g., disproportionation).

(41) The generation of superoxide via autoxidation of ferrous porphyrin is rather slow, so that larger i_r/i_{cat} ratios (≥0.1) can be plausibly caused only by H_2O_2.
(42) Huie, R. E.; Neta, P. In *Reactive Oxygen Species in Biological Systems: An Interdisciplinary Approach*; Gilbert, D. L., Colton, C. A., Eds.; Kluwer: New York, 1999; pp 33−63.
(43) Jovanovic, S. V.; Steenken, S.; Tosic, M.; Marjanivic, B.; Simic, M. G. *J. Am. Chem. Soc.* **1994**, *116*, 4846.
(44) Bielski, B. H. J. In *Oxy Radicals and Their Scavenger Systems*; Cohen, G., Greenwald, R. A., Eds.; Elsevier: New York, 1983; Vol. 1, pp 1−7.
(45) Dikalov, S.; Khramtsov, V.; Zimmer, G. *Arch. Biochem. Biophys.* **1996**, *326*, 207.

Antioxidant-modified films of the Cu-free catalysts generated higher i_r/i_{cat} ratios than similar films without antioxidants (Table 1, entries 3−6). The magnitude of this increase correlated with the reported rates of superoxide reduction by these antioxidants. In control experiments, mixed films containing inert additives structurally similar to the employed antioxidants displayed the i_r/i_{cat} ratios only slightly higher than those of the unmodified films (Table 1, entries 7−9). The maximum antioxidant-induced increase in the i_r/i_{cat} ratio (2-fold, entry 6) implies that O_2^-/HO_2 is the major PROS generated by the Cu-free catalysts at 250−50 mV. If this interpretation is correct, the apparent autoxidation rate of a dioxygenated Cu-free catalyst is ∼0.03 s^{-1}, and its minimum selectivity toward *4e* O_2 reduction is ∼90%.[37] In contrast, the dilution of the FeCu catalyst with the antioxidants did not increase i_r/i_{cat}, indicating that the steady-state O_2^- concentration generated by the bimetallic catalyst is below our detection limit.

The incorporation of H_2O_2 scavengers (i.e., ebselen[46] or thiourea[47]) into catalytic films does not affect the i_r/i_{cat} ratios (entries 8 and 9). The result is, however, ambiguous because the relatively slow reactions of H_2O_2 with organics probably makes them kinetically noncompetetive with H_2O_2 diffusion out of the film.

Stability of Catalysts. The turnover numbers (TNs, mol O_2/mol catalyst), which quantify the stabilities of our catalysts during turnover, were measured both at a physiologically relevant potential (200 mV) and in the plateau region (≤−100 mV). The estimated TNs are only lower limits because, to simplify calculations, we treated all electroactive catalysts as equally able to participate in catalysis and assumed that the partial degradation of the catalytic film during prolonged O_2 reduction does not change the physical properties of the film so as to block a nondegraded catalyst from participating in catalysis.

At 200 mV, decomposition of the catalysts is accompanied by increased PROS leakage (decreased catalytic selectivity); the TNs under these conditions specify the moles of O_2 reduced to H_2O by one mole of the catalyst without measurable loss of selectivity. The TNs were estimated from an increase in the i_r/i_{cat} ratio after the catalyst was polarized at 200 mV in the presence of O_2 for the desired period of time (∼10 min). The similar TNs of the FeCu ($1.2(2) \times 10^4$) and Fe-only ($1.1(5) \times 10^4$) catalysts are independent of both O_2 tension and pH (below 8).

The catalysts are significantly less stable in O_2 reduction at $E \leq -100$ mV.[26] The temporal evolution of i_{cat} generated by a catalytic film with $\Gamma_t \geq 1$ nmol/cm^2 polarized at a constant potential is adequately described by a KL equation with a time-dependent kinetic ($1/i_k$) term (eq 1):

$$\frac{1}{i_{cat}} = \frac{1}{i_L} + \frac{1}{i_k}(1 + \alpha t^{1/2})e^{C(t)/(4F\beta)} \qquad (1)$$

Here, α ($s^{-1/2}$) and β ((mol O_2)$^{-1}$) are empirical constants which depend on Γ_t, $C(t)$ is the amount of current (Coulombs) passed by time t, and i_L and i_k are the Levich current for the *4e* O_2 reduction and the kinetic current for a fresh film ($t = 0$), respectively. The fall of the catalytic current with time results not from the decreasing redox stoichiometry of the O_2 reduction (which remains ∼*4e*/O_2) but from diminished catalytic activity (smaller i_k). The decrease in the latter described by the ($1 + \alpha t^{1/2}$) term is completely reversible (within 10 s after polarization is stopped) and is probably associated with physical changes in the constantly polarized catalytic film rather than with the chemical decomposition of the catalyst. The pseudo-first-order rate law of the irreversible loss of catalytic activity (the exponential term) indicates that the degradation rate is proportional to the amount of *degraded* catalyst. This suggests that the decomposition of the intact catalyst is caused mainly by reactive species generated by the partially degraded catalytic film. At −100 mV in air-saturated pH 7 buffer, the TNs at 50% decomposition of the FeCu and Fe-only catalysts are $2.1(9) \times 10^3$ and $7(2) \times 10^2$, respectively.

Table 2. Current Densities (mA/cm^2) of the Catalytic Reaction (j_k), Charge (j_c), and Reactant (O_2/H_3O^+/Buffer, j_S) Transfers in Films with $\Gamma_t = 2.5$ nmol/cm^2

	FeCu	Fe-only	ZnCu
j_c[a]	30(2)	45(2)	
j_S[b,c]			25(9)
j_k[c,d] (at $E_{1/2}$)	0.14(2)	0.14(3)	
j_k[c,d] (at plateau)	11.2(3)	6.0(3)	

[a] Calculated by eq 2 in ref 50 from transient potential step measurements in the absence of a substrate and assuming a largely isotropic film of uniform thickness. [b] Extrapolated from the value for O_2 reduction at EPG modified with 25−50 nmol/cm^2 of the catalytically inactive ZnCu analogue of the FeCu catalyst. [c] In air-saturated electrolyte (O_2 concentration of 0.24 mM). [d] From the intercepts of the Koutecky−Levich plots.

The reaction of many simple Fe porphyrins with H_2O_2 results in O−O bond homolysis, generating highly destructive free hydroxyl radicals (Fenton chemistry).[48,49] Free •OH cannot be detected by the ring electrode because once generated they rapidly oxidize any reducible components of the catalytic film, such as the porphyrin macrocycle, leading to catalyst bleaching. Thus, TNs of a catalyst that induces O−O bond homolysis would be higher in the presence of •OH scavengers. We employed mannitol, azide, and carnosine, which do not inhibit our catalysts and are commonly used in biochemical experiments as •OH scavengers.[47] In O_2 reduction at 200 mV, the presence of these scavengers in the electrolyte does not affect the stability of either catalyst. In contrast, an ∼30% increase in TNs is observed if O_2 reduction at −100 mV is conducted in the presence of mannitol (>10 mM).

Kinetic Mechanism of O_2 Reduction. The overall rate of catalysis in a multilayer catalytic film may be limited not only by the rate of the catalytic reaction but also by the rate of charge transfer within the film and/or of substrate transfer from the solution−film interface to the active sites. The comparison of the intercepts of the Koutecky−Levich plots with the specific current densities for charge and substrate transfer within the catalytic films, measured independently, (Table 2) indicates that the turnover-limiting process is the catalytic reaction. The Koutecky−Levich dependence of the catalytic currents on electrode rotation frequency serves as additional evidence that

(46) Sies, H. *Methods Enzymol.* **1994**, *234*, 476.
(47) Halliwell, B.; Gutteridge, J. M. C. *Methods Enzymol.* **1990**, *186*, 1.
(48) Watanabe, Y. In *The Porphyrin Handbook*; Kadish, K. M., Smith, K. M., Guilard, R., Eds.; Academic Press: San Diego, CA, 2000; Vol. 4, pp 97−117.
(49) Weiss, R.; Gold, A.; Trautwein, A. X.; Terner, J. In *The Porphyrin Handbook*; Kadish, K. M., Smith, K. M., Guilard, R., Eds.; Academic Press: San Diego, CA, 2000; Vol. 4, pp 65−96.
(50) Anson, F. C.; Tsou, Y.-M.; Saveant, J.-M. *J. Electroanal. Chem.* **1984**, *178*, 113.

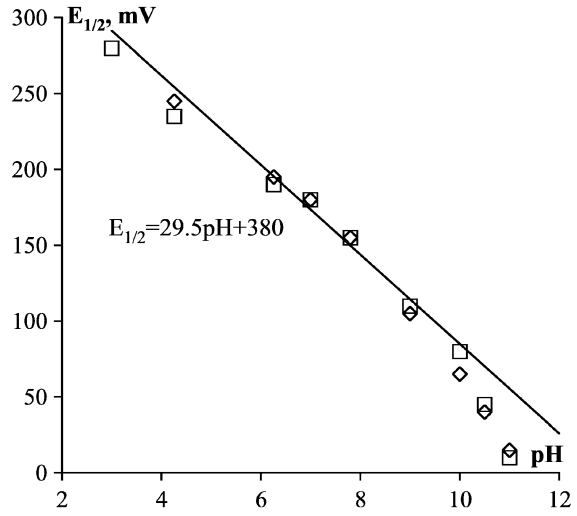

Figure 7. pH dependence of catalytic half-wave potentials ($E_{1/2}$, air-saturated electrolytes at 200 rpm) for the FeCu (◊) and Fe-only (□) catalysts. The solid line: a linear least-squares fit to the equation shown (using data at pH < 9).[26]

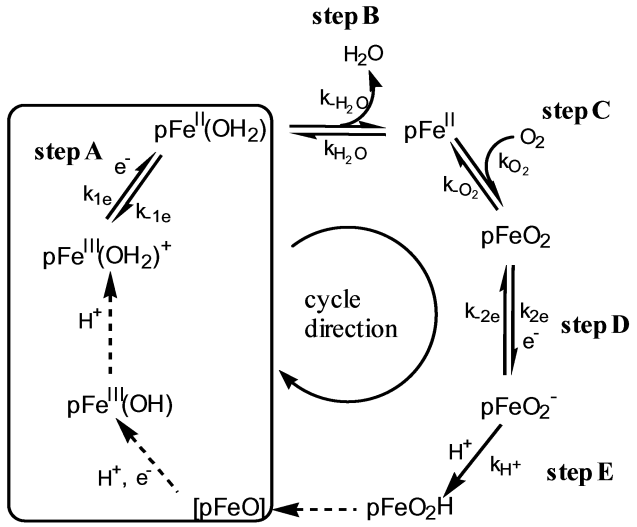

Figure 8. Kinetic mechanism of O_2 reduction at the rising part of the catalytic wave at pH < 9. The chemical formulas describe composition and do not imply any particular structure. The transformations depicted by the broken errors are kinetically "invisible" under these conditions. Boxed steps were studied independently by CV under N_2. Data on step B are available from inhibition studies.[32] Two reversible ET steps (A and D) and the turnover-determining protonation (step E) account for the −30 mV/pH dependence of the half-wave potentials. At pH > 9, the "resting" state of the catalyst becomes $pFe^{III}(OH)$, which leads to the change in the $E_{1/2}$(pH) gradient.[26]

the charge transfer is substantially faster than the catalytic turnover.[51] Likewise, the direct proportionality of the Koutecky−Levich intercepts to the amount of the deposited catalyst (at $\Gamma_t \leq 2.5$ nmol/cm^2)[26] is inconsistent with the substrate transfer being turnover-limiting, in which case the inverse proportionality would be observed.[52]

The pH dependence of the half-wave potentials, $E_{1/2}$, and of the limiting kinetic currents is commonly studied to understand the kinetic mechanism of electrocatalytic processes.[53] We find that, at pH < 9 both the FeCu and Fe-only catalysts display a similar −29.5(9) mV/pH shift of the half-wave potentials (Figure 7). The identical $E_{1/2}$ values for the two catalysts strongly suggest that Cu does not significantly affect the kinetic mechanism. An ∼−30 mV/pH gradient is unusual in electrocatalytic O_2 reductions[22,53] and indicates that the turnover-determining part of the catalytic cycle contains two reversible electron-transfer (ET) steps and a protonation. The limiting kinetic currents were pH-independent.

The kinetic currents are first order in both the catalyst and O_2.[26] In such a case, the kinetics of a catalytic cycle can be analyzed qualitatively within a noncyclical linear reaction sequence, starting with the resting form of the catalyst under the given conditions and ending with the turnover-determining step (TDS).[54] As was shown earlier (Figure 3), the "resting" state of the catalyst at pH < 9 and potentials around $E_{1/2}$ is ferric-aqua, $pFe^{III}(OH_2)^+$. A *1e* reduction to the ferrous state and a dissociative loss of H_2O, yielding the catalytically active five-coordinate pFe^{II}, are required for the formation of the obligate catalyst−substrate complex (oxy-Fe porphyrin, $pFeO_2$, Figure 8). The additional reversible electron-transfer step and protonation necessary to give the observed ∼−30 mV/pH shift in $E_{1/2}$ must occur after the generation of this $pFeO_2$ adduct. Thus, the chemical composition of the intermediate involved in the TDS is $pFe^{III}(O_2H^-)$, a formally ferric-hydroperoxo adduct. Between the two conceivable sequences, (1) a reversible reduction of $pFeO_2$ to $pFeO_2^-$ followed by turnover-determining protonation (Figure 8) or (2) a reversible formation of $pFeO_2H$ that is consumed in an irreversible step without a proton or an electron uptake, the latter is less likely. Extensive research on the reactivities of iron porphyrins with H_2O_2[48,49] indicates that the double protonation of the distal oxygen or a concerted transfer of a second H^+ is necessary for the O−O bond heterolysis, whereas homolysis dominates the decomposition of a monoprotonated peroxo-level adduct ($pFeO_2H$). We see no evidence of O−O bond homolysis in O_2 reduction at the potential-dependent part of the catalytic waves. When concerted with O−O bond heterolysis, H^+ transfer from a buffer molecule to the $pFeO_2H$ intermediate would not affect the pH dependence of $E_{1/2}$. This possibility, however, is ruled out by the observation of an ∼−30 mV/pH gradient in unbuffered solutions at pH ≤ 5[55] and by the lack of rate dependence on the nature of the buffer.

The generation of $pFeO_2H$ in the TDS minimizes the steady-state concentration of this intermediate and, hence, the H_2O_2 flux into bulk medium, since the dissociative decomposition of $pFeO_2H$ is the most likely source of H_2O_2 in metalloporphyrin-catalyzed O_2 reduction.[22] O_2 reduction at the heme/Cu site (Figure 2) has been proposed to proceed via a similar kinetic sequence.[17] In contrast to our catalysts, O_2 reduction at other metalloporphyrins appears to proceed via O_2 binding as the TDS.[22,56] The difference may be due to the imidazole ligation

(51) Andrieux, C. P.; Saveant, J.-M. In *Molecular Design of Electrode Surfaces*; Murray, R. W., Ed.; Wiley: New York, 1992; Vol. 22, pp 207−270.
(52) Kobayashi, N.; Nishiyama, Y. *J. Electroanal. Chem.* **1984**, *181*, 107.
(53) Conway, B. E.; Bockris, J. O. M.; Yeager, E.; Khan, S. U. M.; White, R. E. *Comprehensive Treatise of Electrochemistry*; Plenum: New York, 1983; Vol. 7.
(54) The TDS is defined as the first irreversible step after substrate binding.
(55) Catalysis in unbuffered pH > 5 electrolytes cannot be studied because the maximum obtainable H^+ flux in such solutions at the electrode rotation frequencies employed in the present work is substantially lower than that necessary to maintain the O_2 reduction rate observed in buffered electrolytes. In unbuffered 3.2 < pH ≤ 5 solutions, the plateau currents are limited by H^+ mass-transport and, as a result, are lower than those observed in buffered solutions of the same acidity. The first ∼50% of the catalytic waves in unbuffered solutions coincide with those measured in buffered electrolytes, as do Tafel plots of these early parts. Thus, a buffer is essential to maintain bulk acidity at the electrode surface, not as a reactant in the catalytic cycle.

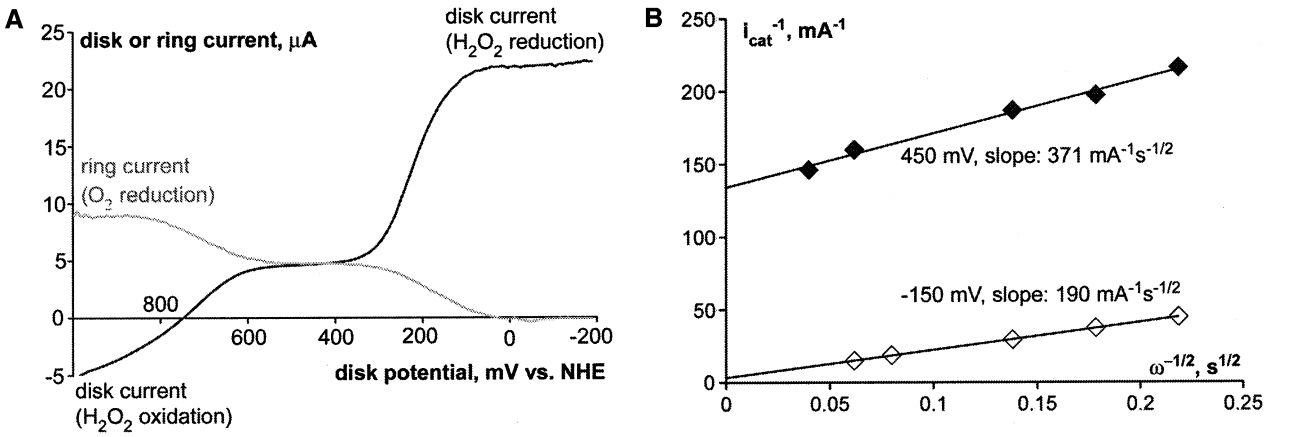

Figure 9. Reduction of H_2O_2 (0.2 mM) in anaerobic pH 7 buffer. (A) An LSV at Au-ring/EPG-disk RRDE; the ring current (gray line) is multiplied by 10 and the collection efficiency of O_2 was 10%. (B) Koutecky−Levich plots for limiting currents at 450 mV (filled points) and −150 mV. The solid lines: the linear least-squares fit to the equations shown. Only the data for the FeCu catalyst are shown; the Fe-only catalyst behaves analogously.

of Fe in our catalysts, which both facilitates the O−O bond heterolysis and increases the O_2 affinity.

A more rigorous mathematical analysis of the kinetic data (given in the Supporting Information) is consistent with the mechanism in Figure 8 and yields eq 2 for the apparent second-order catalytic rate constant. At potentials around $E_{1/2}$, both redox pre-equilibria are sufficiently unfavorable, so that the rate constant depends directly on $[H^+]$ and exponentially on twice the electrochemical potential. At more reducing potentials, these pre-equilibria become so favorable that the terms in parentheses reduce to 1, yielding the expression for the limiting kinetic currents (eq 3).[57]

$$\frac{1}{k_{app}} = \underbrace{\left(1+\frac{k_{-1e}}{k_{1e}}\right)}_{\text{step A}}\underbrace{\frac{k_{H_2O}}{k_{-H_2O}}}_{\text{step B}}\frac{1}{k_{O_2}}\left(k_{-O_2}\frac{k_{-2e}}{k_{2e}}\frac{1}{[H^+]k_{H^+}}+1\right) \qquad \text{eq. 2}$$

$$i_k = nFA\Gamma_t[O_2]_\infty k^l_{app} = nFA\Gamma_t[O_2]_\infty\left(\frac{k_{-H_2O}}{k_{H_2O}}k_{O_2}\right) \qquad \text{eq. 3}$$

According to eq 3 these currents are pH-independent, in line with our experimental observations, and are determined by fractionation between the five- and six-coordinate (aqua) ferrous catalysts (k_{-H_2O}/k_{H_2O}) and the rate of O_2 binding. Although the k_{-H_2O}/k_{H_2O} value for the FeCu catalyst could not be determined, that for the Fe-only catalysts (0.007) is known from inhibition studies.[32] From this value and the apparent limiting catalytic rate constant for Fe-only ($5.1 \times 10^4\ M^{-1}\ s^{-1}$, see "$O_2$ reduction at pH 7" earlier), the rate constant of O_2 binding to the five-coordinate Fe^{II} center in the Fe-only complex, k_{O_2}, is estimated as $7 \times 10^6\ M^{-1}\ s^{-1}$. This is comparable to O_2 binding rate constants for many myoglobins, hemoglobins, and some synthetic superstructured Fe porphyrins containing nitrogenous axial ligands[58] but is an order of magnitude lower than that reported for cytochrome oxidase.

The mechanism in Figure 8 is also consistent with the observed decrease in the i_r/i_{cat} ratio at more reducing potentials. As shown earlier, the small ring current at the potential-dependent portion of the catalytic wave (Figure 4) results primarily from superoxide-releasing autoxidation of the oxygenated catalyst, $pFeO_2$. The concentration of $pFeO_2$ (and hence the O_2^- flux) decreases at more reducing potentials because the TDS changes from protonation of $pFeO_2^-$ at the potential-dependent part of the catalytic wave to O_2 binding at the plateau.

H_2O_2 Reduction. The reactivities of both the FeCu and Cu-free catalysts toward H_2O_2 are very similar. They were studied under N_2 using an Au-ring/EPG-disk RRDE. In this setup, the Au-ring electrode (which is inert to H_2O_2), set at a reducing potential, was used to detect the production of O_2 by the catalytic films. H_2O_2 oxidation (anodic currents at $E > 780$ mV) as well as H_2O_2 reduction by the oxidized ($780 < E < 300$ mV) and reduced ($E < 200$ mV) catalysts give the disk wave (Figure 9). The cathodic ring current between 800 and 50 mV reveals that both the reduction and dismutation of H_2O_2 occur in the film. The i_r/i_{cat} ratios indicate that, at 600−350 mV, overall rates of these two reaction pathways are similar and that disproportionation contributes ~40% to O_2 flux generated at 1000−800 mV. The decrease in the ring current below 200 mV may be caused by O_2 reduction becoming faster than its diffusion out of the film, by H_2O_2 reduction at ferrous centers becoming faster than its oxidation by high-valent Fe species (e.g., oxoferryl porphyrin cation-radical), or by a combination of these processes.

At 780 mV (zero-current potential at pH 7), O_2 is generated solely by H_2O_2 dismutation; the ring current is directly proportional to the bulk H_2O_2 concentration and corresponds to an apparent second-order rate constant for catalytic H_2O_2 disproportionation $\geq 1.4(2) \times 10^3\ M^{-1}\ s^{-1}$. This value is the largest ever reported for a synthetic Fe porphyrin and is ~100 times larger than that of myoglobin under comparable conditions.[29,31,59−62] This observation illustrates how efficient our complexes are at inducing O−O bond heterolysis, consistent with the low lifetime of the ferric-hydroperoxo adduct postulated from the analysis of the kinetic data (see earlier).

The catalytic currents at plateaus of both waves exhibit the Koutecky−Levich behavior; the limiting currents of the second wave yield the KL slope equal to that calculated for *2e* H_2O_2 reduction. A parallel H_2O_2 disproportionation evident in the RRDE experiments accounts for the greater KL slope at the

(56) Shigehara, K.; Anson, F. C. *J. Phys. Chem.* **1982**, *86*, 2776.
(57) In eq 3, $n = 4$ is the redox stoichiometry of O_2 reduction, F is the Faraday constant, A is the geometric area of the electrode, $[O_2]_\infty$ is the bulk O_2 concentration; k^l_{app} is the *limiting* rate constant. To simplify calculations, we took the coefficient of O_2 partitioning between the film and electrolyte as 1; the precise value of this coefficient does not affect the mechanistic conclusions.
(58) Momenteau, M.; Reed, C. A. *Chem. Rev.* **1994**, *94*, 659.

Table 3. Summary of the Electrocatalytic Properties of the Heme/Cu Analogues in the FeCu and Fe-only Forms and Relevant Data for Cytochrome Oxidase

entry	substrate	parameter	FeCu	Fe-only	enzyme
1	O_2 (0.21 atm)	$E_{1/2}$, mV	190	190	
2		min. selectivity,[a] %	>96−98	>90	
3		k_{app}(200 mV), $M^{-1}\,s^{-1}$	630	580	
4		$(k_{app})_{max}$, $M^{-1}\,s^{-1}$	1.2×10^5	5.1×10^4	$1.5-2.5 \times 10^{5\,b}$
5		k_{O_2}, $M^{-1}\,s^{-1}$		7×10^6	$1-3 \times 10^{8\,b}$
6		TN (200 mV)	1.2×10^4	1.1×10^4	
7	H_2O_2 (0.2 mM)	$E_{1/2}$, mV	160	155	
8		k_{app} (450 mV), $M^{-1}\,s^{-1}$	800	350	700[c]
9		$(k_{app})_{max}$, $M^{-1}\,s^{-1}$	1.7×10^4	1.0×10^4	$2 \times 10^{4\,d}$
10		TN	460	240	
11		+mannitol (10 mM)	460	340	
12	none	$E°$, mV	120	100	≥250[e]

[a] The fraction of the *4e* pathway calculated from the maximum collection-efficiency corrected i_r/i_d ratios (0.031 for Fe-only and 0.011 for FeCu) using the equation in ref 37. [b] References 4 and 5 (higher value). [c] Reference 4. [d] Single-turnover experiment, ref 4. [e] The heme a_3/Cu_B potential depends both on the site's protonation state[72a] and on the redox states of heme a and Cu_A,[72b] and it may be higher or lower[72a] than indicated.

first wave because it depletes H_2O_2 at the electrode surface without contributing to the catalytic current. The ratio of the two slopes (1.95) indicates similar overall rates for H_2O_2 reduction and disproportionation, in accord with the results of the RRDE experiments. H_2O_2 reduction by the ferrous catalyst is ∼25 times faster than that by the ferric analogue. A similar difference in reactivities has been observed for cytochrome oxidase.[4] In contrast, the previously reported synthetic Fe porphyrins were inert toward H_2O_2 in the ferric state on the time scale of an electrocatalytic experiment.[22,56]

The TNs in H_2O_2 reduction were determined analogously to those in O_2 reduction at the plateau. Catalytic H_2O_2 reduction is accompanied by a much faster catalyst decomposition than that observed during O_2 catalysis (e.g., $4.6(2) \times 10^2$ vs $1.2(2) \times 10^4$ for the FeCu catalyst). At pH > 5, the TNs of the Fe-only catalyst increase up to 2-fold in the presence of •OH scavengers, and the magnitude of the increase correlates with the scavenger concentration. These data strongly suggest that H_2O_2 reduction by the Fe-only catalyst is accompanied by some O−O bond homolysis. The TNs at pH 3 are 3-fold higher than those at pH 7 and are insensitive to the presence of •OH scavengers. This is consistent with a more facile protonation of the distal oxygen in coordinated peroxide at a lower pH, which favors O−O bond heterolysis over the •OH-generating homolysis. The TNs of the more stable FeCu catalyst are unaffected by •OH scavengers, so that FeCu may not generate •OH. This may result from Cu-induced polarization of the O−O bond, which is known to favor the heterolytic cleavage.[48]

Discussion

We investigated electrocatalytic reductions of O_2 and H_2O_2 by a series of synthetic analogues of the heme/Cu site of terminal oxidases. These catalysts are the closest mimics of the heme/Cu site yet reported. They reproduce the trisimidazole coordination of the distal Cu, the imidazole proximal ligand of the Fe, and the FeCu separation (Figure 1) of the heme/Cu site as well as its reactivity under noncatalytic conditions.[23,63] Because of yet-unsolved synthetic problems, our present analogues do not incorporate a phenol moiety in the second coordination sphere of Cu. However, recent work by Wikström et al. convincingly shows that the phenol is not involved in the catalysis by the fully reduced enzyme.[15] Herein, we studied the steady-state catalysis under fast electron flux (Table 2), which is equivalent to a single turnover by the fully reduced enzyme (the electrode mimicks reduced Cu_A and heme a). Under these conditions, the absence of the phenol residue is not expected to significantly alter the reactivity of the FeCu core.

The data presented in the Results section establish that our heme/Cu analogues reproduce several important aspects of cytochrome oxidase's reactivity. First, they catalyze the *4e* reduction of O_2 at physiologically relevant potentials without significant PROS release (Table 3, entries 1 and 2). Second, this reduction proceeds without a buildup of the hydroperoxo intermediate. Third, the maximum (e.g., measured at the plateau) catalytic rate constants for O_2 reduction as well as H_2O_2 reduction by the oxidized and reduced FeCu catalyst are comparable to those reported for cytochrome oxidase (Table 3, entries 4, 8, 9). In addition, our synthetic analogues manifest catalase activity as does cytochrome oxidase.

A two-step mechanism was proposed[56,64] to account for the *4e* activity of some simple Fe porphyrins adsorbed on a graphite electrode, whereby H_2O_2 generated during O_2 reduction is catalytically dismutated (or reduced to H_2O) by neighboring molecules of the metalloporphyrin before it can diffuse into the bulk medium. Our data indicate that this biologically irrelevant mechanism is unlikely to operate in our systems. First, in contrast to the case of other Fe porphyrins, the kinetics of O_2 reduction by our complexes (Figure 8) is such that the steady-state concentration of the intermediate most likely to release H_2O_2 ($pFeO_2H$) is minimized. Within this mechanism, the observed small i_r/i_{cat} ratios are inconsistent with the intermediacy of free H_2O_2. Second, at pH 7, the TNs in O_2 reduction at ∼200 mV are 25−50 times higher than the TNs for H_2O_2 reduction under comparable conditions (Table 3, entries 6 and 10). This

(59) Most literature data are formation rates of $(por^{+\bullet})Fe^{IV}{=}O$ (O−O bond heterolysis) and/or $(por)Fe^{IV}{=}O$ (O−O bond homolysis) from a ferric porphyrin and H_2O_2. The corresponding rate constants vary from 22(5) $M^{-1}\,s^{-1}$ or 190 $M^{-1}\,s^{-1}$ for ClFe(F20TPP) in $MeOH/CH_2Cl_2$[31,60] to 900 $M^{-1}\,s^{-1}$ for sulfonated bisortho-substituted TPP derivatives in water.[29] The overall rate constant of H_2O_2 disproportionation cannot exceed these values because $(por^{+\bullet})Fe^{IV}{=}O$ oxidizes H_2O_2 to O_2. With the exception of catalases, the overall rate of H_2O_2 dismutation is much slower than that of $(por^{+\bullet})Fe^{IV}{=}O$ formation. For example, in Mb and met-Mb, the corresponding rate constants are 3600 $M^{-1}\,s^{-1}$ and 440 $M^{-1}\,s^{-1}$, respectively,[61] and the dismutation rate constant is 15 $M^{-1}\,s^{-1}$.[62]

(60) Cunningham, I. D.; Danks, T. N.; O'Connell, K. T. A.; Scott, P. W. *J. Chem. Soc., Perkin Trans. 2* **1999**, 2133.

(61) Shikama, K. *Chem. Rev.* **1998**, *98*, 1357.

(62) Adachi, S.; Nagano, S.; Ishimori, K.; Watanabe, Y.; Morishima, I.; Egawa, T.; Kitagawa, T. *Biochemistry* **1993**, *32*, 241.

(63) Collman, J. P.; Sunderland, C. J. Manuscript in preparation.

(64) Shi, C.; Anson, F. C. *Inorg. Chem.* **1990**, *29*, 4298.

puts an upper limit of $<2-4\%$ on the fraction of O_2 reduced to H_2O through the intermediacy of free H_2O_2 under these conditions. Finally, electrocatalysis in the presence of $^{\bullet}OH$ scavengers shows that the exposure of these catalysts to H_2O_2 (either as the primary substrate or as a product of side reactions) yields free $^{\bullet}OH$. The same method failed to reveal the generation of $^{\bullet}OH$ in O_2 reduction at $\sim$200 mV.

On the basis of both the structural and functional fidelities of our catalysts as analogues of the heme/Cu site of terminal oxidases, the comparison of the catalytic behaviors of the FeCu and Cu-free complexes suggests how Cu_B in cytochrome oxidase may affect the reactivity of the heme toward O_2 and H_2O_2. First, we find that, in the regime of rapid electron flux, Cu does not influence the rate, the kinetic mechanism of the catalysis, or the catalyst stability (Table 3, entries 3 and 6). We have shown elsewhere that Cu is essential for catalytic activity under diffusion-limited electron flux.[65] As these effects are observed only when electron delivery is slower than the catalytic reaction, we conclude that Cu^I in the trisimidazole environment acts mainly as a *1e* storage site apparently without providing a lower-energy pathway relative to O_2 reduction at an (por)Fe alone. These findings contrast with recent computational studies of the O−O bond cleavage at the heme/Cu site of cytochrome oxidase, which identified the energetically preferred pathway as hydrogen atom transfer from Cu_B^I-coordinated H_2O to form the ferric-hydroperoxo intermediate (Figure 2). The mechanism of this step may be very sensitive to proton availability at the catalytic site, which is difficult to reproduce either biomimetically or computationally, so that differentiating between these two alternative sequences requires further studies.

Under fast electron flux, the most notable effect of Cu on the reactivity of our heme/Cu analogues is the suppression of superoxide-releasing autoxidation of the oxygenated catalyst. Experiments with O_2-reductants incorporated into catalytic films indicate that the Cu-free catalysts autoxidize at an apparent rate constant of $\sim 0.03\ s^{-1}$, whereas autoxidation of the FeCu catalysts under these conditions is at least 10 times slower. In the past, O_2^- -releasing autoxidation has not been considered as the major PROS source in the electrocatalytic O_2 reduction by Fe porphyrins. Although unfavorable at physiologically relevant potentials, this reduction of O_2 to O_2^- is driven by subsequent rapid irreversible reactions, such as the disproportionation of O_2^- to O_2 and H_2O_2.[66] Under aerobic conditions, all known ferrous porphyrins that bind O_2 reversibly (including hemoproteins) generate superoxide by the heterolytic decomposition of the O_2 adduct (autoxidation).[62] For heme enzymes, apparent autoxidation rate constants in air-saturated pH 7 buffers vary from $<10^{-6}\ s^{-1}$ for myoglobin to $\sim 0.03\ s^{-1}$ for indoleamine dioxygenase.[7,8,67] Some $Fe^{II}N_4$-macrocyclic complexes autoxidize 10−20 times faster.[62] The mechanism of autoxidation is not well established, but the protonation of the FeO_2 moiety is known to lead to its rapid dissociation into HO_2 and ferric porphyrin. This process is greatly facilitated by ionizable groups in the O_2-binding pocket that are capable of proton transfer to the terminal oxygen.

Hence, H^+ transfer from a protonated distal imidazole of the Fe-only catalyst to the terminal oxygen of the FeO_2 moiety may account for the relatively rapid autoxidation of the Cu-free catalysts. In the FeCu catalyst, Cu would block this proton-relay mechanism by forming coordination bonds with the basic N atoms of the distal imidazoles. Comparable selectivities of the Fe-only and FeZn analogues may be due to the transient dissociation of one of the imidazoles from Zn^{2+}, which frees it for H^+ relay. This hypothesis is suggested by the crystal structure of a structurally related Zn-containing imidazole-picket porphyrin, wherein Zn is coordinated to only two imidazoles.[25a] Alternatively, Cu may recapture the released superoxide and transfer it back to Fe. A much faster autoxidation of the Fe-only complex relative to the FeCu analogue is also observed in oxygenated aprotic solvents under stoichiometric conditions.[63]

The Cu_B-induced stabilization of oxyheme against autoxidation may be biologically beneficial. If the reduction of compound A (Figure 2) requires hydrogen atom transfer as is currently thought, the protonation of the bound O_2 appears as a likely side reaction. Analysis[62] of the myoglobin autoxidation rates suggests that HO_2 dissociation from protonated oxyhemes may occur at a rate comparable to the O_2 off-rate; the latter is $>10^4\ s^{-1}$ in cytochrome oxidase.[2,5] The superoxide-releasing decomposition of compound A would increase the flux of toxic O_2 metabolites and could also decrease the proton pump efficiency. The amount of O_2 eliminated by a few percent increase in the catalytic selectivity of O_2 reduction achieved through the Cu-induced suppression of autoxidation may be comparable to the total O_2 flux generated within normally functioning mitochondria ($\sim$1−2% of O_2 consumption). The latter process is the major intracellular source of PROS,[68] and its magnitude is large enough to warrant the existence of an extensive mitochondrial superoxide defense system, particularly in the form of a high Mn superoxide dismutase concentration.[69]

The higher limiting catalytic rate constants of the FeCu catalyst relative to the Cu-free analogues (Table 3, entry 4) are likely due to the acceleration of O_2 binding by Cu. Such acceleration is observed in related complexes under stoichiometric conditions.[70] O_2 binding to cytochrome oxidase appears to proceed through transient coordination to Cu_B, although it is not established whether it accelerates the formation of compound A.[2,5] Finally, Cu also appears to suppress O−O bond homolysis during H_2O_2 reduction, which is evidenced from the difference in the relevant turnover numbers of the FeCu and Cu-free catalysts measured in the presence and absence of $^{\bullet}OH$ scavengers (Table 3, entries 10 and 11). The result may be due to the electrostatic polarization of the O−O bond by Cu, which would favor heterolysis.

While our complexes reproduce key aspects of the heme/Cu reactivity, they are comparatively slow catalysts at physiologically relevant potentials (entry 3), probably as a result of a relatively hydrophilic environment around the biomimetic catalyst in direct contact with an aqueous electrolyte. First, this substantially increases the population of the catalytically inactive ferrous-aqua form. Second, the more efficient charge stabilization decreases the $Fe^{III}Cu^{II}/Fe^{II}Cu^{I}$ potential relative to that of the heme/Cu site by over 100 mV (entry 12).[27] Hence, better

(65) Collman, J. P.; Boulatov, R. *Angew. Chem., Int. Ed.* **2002**, in press.
(66) Stanbury, D. M.; Haas, O.; Taube, H. *Inorg. Chem.* **1980**, *19*, 518.
(67) Brantley, R. E.; Smerdon, S. J.; Wilkinson, A. J.; Singleton, E. W.; Olson, J. S. *J. Biol. Chem.* **1993**, *268*, 6995.
(68) Chance, B.; Sies, H.; Boveris, A. *Physiol. Rev.* **1979**, *59*, 527.
(69) Gilbert, D. L.; Colton, C. A. *Reactive Oxygen Species in Biological Systems: An Interdisciplinary Approach*; Kluwer: New York, 1999; Chapters 3 and 7.
(70) Collman, J. P.; Berg, K. E.; Sunderland, C. J.; Shiryaeva, I. M. To be reported.

reproduction of the relatively hydrophobic environment of the protein matrix in the vicinity of the heme/Cu site may yield biomimetic catalysts with a specific activity exceeding that of cytochrome oxidase.

Conclusion

In this work, we have established that new biomimetic complexes with a significant structural similarity to the heme/Cu site of terminal oxidases also reproduce key aspects of these enzymes' reactivity. The catalytic reductions of O_2 and H_2O_2 in an aqueous medium were studied voltammetrically. The biomimetic complexes were adsorbed on the surface of a graphite electrode, which served as an outer-sphere electron-transfer agent not dissimilar to cytochrome *c*. These synthetic heme/Cu analogues reduce O_2 with a high selectivity under physiologically relevant conditions. The formally ferric-hydroperoxo intermediate is generated in the turnover-determining step, which minimizes its steady-state concentration and, hence, the flux of H_2O_2 formed by its decomposition. The maximum catalytic rates are comparable to those reported for cytochrome oxidase, and the biomimetic complexes manifest notable catalase activity.

The structural and functional fidelities of our catalysts as heme/Cu mimics allowed us to probe, for the first time ever, the structure/function relationship within the catalytic site of cytochrome oxidase using biomimetic chemistry. We find that, in the regime of rapid electron flux, Cu does not affect the kinetics of the catalysis or the stability of the catalysts. This is consistent with the role of Cu_B in cytochrome oxidase as mainly an electron storage site, similar to heme a or Cu_A. Our data suggest that Cu_B may not provide a unique pathway for O−O bond reduction that would not be accessible if the catalytic site of cytochrome oxidase was made up of the heme alone. However, Cu affects the reactivity of the heme/Cu analogues by nonredox mechanisms. Most notably, Cu suppresses superoxide-releasing autoxidation of oxygenated catalyst, thereby decreasing the flux of partially reduced oxygen species during steady-state O_2 reduction. Cu also accelerates O_2 binding and minimizes O−O bond homolysis in the reduction of H_2O_2.

Experimental

Materials and Equipment. The synthesis and characterization of the complexes have been described elsewhere.[23] Catalytic films were prepared using the catalysts oxidized in air either in the solid state or as methanol solutions. The oxidized (Fe^{III} or $Fe^{III}Cu^{II}$) complexes generate single peaks in the electrospray mass spectroscopy corresponding to the molecular ions of the intact complexes. Such complexes give analytically uninformative ^1H and ^{19}F NMR or EPR spectra, but they can be reduced with CO to yield diamagnetic NMR spectra corresponding to those of the reduced complexes synthesized directly. CO is routinely used to reduce the heme/Cu site of terminal oxidases. Monitoring the oxidation of methanol solutions of the complexes in air by UV-vis spectroscopy reveals isosbestic behavior between two chromophores corresponding to the reduced and oxidized complexes. This confirms that the oxidation proceeds without significant decomposition of the porphyrin ligand, which would result in appearance of additional chromophores.

Air used in the electrochemical experiments was scrubbed for CO_2 by passing it through two traps with 2 M NaOH solutions, followed by a trap with water. Other O_2 tensions were obtained by using commercially available O_2−N_2 mixtures (Air Products, Inc.). Water was purified with a NANOpure II unit and had a conductivity > 18.3 MOhm/cm. All reagents/solvents were of the highest purity commercially available. The supporting electrolyte (KPF_6) was recrystallized at least twice from a basic solution (pH 10); the pH of ~0.5 M solutions of recrystallized KPF_6 was 6.9(2), and this solution displayed a single ^{19}F NMR peak.

The electrochemical experiments were carried out in custom-made cells (250 mL) with an outer jacket for thermostating the aqueous electrolyte and a tightly fitting Teflon lid. In the RRDE experiments, the cell was placed in a grounded homemade Faraday cage.

A BAS CV-50W potentiostat (Bioanalytical Systems) and a Pine AFCBP1 bipotentiostat (Pine Instruments) were used for rotating disk and ring−disk experiments, respectively; speed controllers were ASR or MSR type (Pine Instruments). A low flowrate calomel electrode and a Pt mesh were used as the reference and auxiliary electrodes, respectively. The working electrodes were an edge-plane graphite (EPG), basal plane or Au rotating disk electrodes or a ring−disk electrode with a removable disk, and a Pt ring or Au ring; all were from Pine Instruments.

The EPG disks (0.195 cm^2) were cleaned with a 600 grit SiC paper and sonicated for 1 min in methanol immediately prior to depositing a catalytic film.

Particular care was exercised to ensure the high reactivity of the Pt ring toward H_2O_2 oxidation and of the Pt-disk electrode used as the *4e* O_2 reduction standard. The theoretical collection efficiency of the RRDEs is 22.5% and was experimentally observed with the $Fe(CN)_6^{3-/4-}$ couple; the efficiencies of the H_2O_2 collection varied between 21 and 14% (at 200 rpm), depending on the buffer. Our own experience and analysis of the literature identify three major sources of Pt fouling in electrochemical biomimetic O_2 reduction: deposition of organics during film preparations, adsorptions from the electrolyte (e.g., of Cl^-) during a catalytic run, and gradual surface aging through other processes. Syringing the catalyst on the disk (as opposed to dip-coating) and the relatively wide disk−ring gap completely eliminate Pt contamination during film preparation. This ensures that N_{per} of the modified electrode is identical to that measured at the beginning and the end of each daily series of RRDE experiments by electrochemical O_2 reduction on a bare disk. Second, carefully purified electrolytes that do not adsorb strongly to Pt were employed; Cl^- contamination of the electrolyte from the reference SCE was mitigated by using a low-flowrate miniature electrode and frequently changing electrolytes. Finally, Pt was cleaned with a 0.05-mm γ-alumina paste for 1 min, followed by sonication in methanol for 1 min immediately prior to use. The electrode was stored in methanol when not in use. Monthly, Pt was polished thoroughly (2−3 h) with alumina paste; every 2−3 months, Pt was cleaned with concentrated HNO_3 overnight. In any cleaning of the Pt ring, the EPG disk was substituted by an all-Teflon insert to avoid the contamination of Pt with graphite particles and to preserve the integrity of the graphite surface.

The concentration of dissolved O_2 in various electrolytes was measured with an Orion 835A oxygen meter and corrected for solution salinity. Conductivities of the electrolytes were measured with a regular conductivity bridge and, whenever necessary, were adjusted to that of the standard pH 7 buffered electrolyte by varying the KPF_6 concentration.

Statistical analysis was performed using the statistical functions of Microsoft Excel and as described elsewhere.[71] Nonlinear least-squares fits were performed with Kaleidagraph.

Procedures. A sample of a catalyst in the reduced form (0.1 μmol) was dissolved in methanol (200 μL) and oxidized in air; the solvent was removed, the solid was redissolved in a dimethoxyethane−water (15%) mixture of a necessary volume to give the desired concentration,

(71) Vogel, A. I. *Vogel's Textbook of Quantitative Chemical Analysis*, 6th ed.; Prentice Hall: Harlow, U.K., 2000.
(72) (a) Verkhovsky, M. I.; Morhan, J. E.; Wikstrom, M. *Biochemistry* **1995**, *34*, 7483. (b) Rich, P. R.; Moody, A. J. In *Bioenergetics*; P. Graber, Milazzo, G., Eds.; Birkhauser: Basel, Switzerland, 1997; Vol. 4, pp 418−456.

and the sample was placed in a microvial. Samples were stored at −22 °C when not in use and were discarded after 5 days in air (to prevent changes in the sample concentration through solvent evaporation; the oxidized complexes are chemically stable in air for at least 1 month).

Unlike most other metalloporphyrins, our catalysts adsorb only weakly on graphite surfaces, probably because the bulky superstructures on both faces of the macrocycle block the necessary $\pi-\pi$ interactions between the porphyrin and graphite. As a result, dip-coating is unsuitable for film preparation. The screening of numerous solvents (CH_2Cl_2, $CHCl_3$, THF, acetonitrile, dioxane, diethoxyethane, methanol, ethanol, and their mixtures) was used to identify the casting solvent that gave the most reproducible results on edge- and basal-plane graphite as well as on gold surfaces. A 1 μL aliquot of a catalyst solution was syringed on a vertically positioned rotating (300 rpm) cleaned (as described earlier) electrode and allowed to evaporate for 2 min in air, followed by 2 min under a stream of N_2.

The complexes can be desorbed off EPG with methanol almost quantitatively; the amount of the desorbed catalyst was determined by UV-vis spectroscopy; no more than ≤10% of the deposited catalyst is lost during a regular set of electrocatalytic measurements.

The nature of neither the supporting electrolyte (KPF_6, KNO_3, $KClO_4$) nor the buffer noticeably affects the electrochemical or electrocatalytic properties of the complexes. We screened the following pH 7 buffers: $KH_2PO_4-Na_2HPO_4$, lutidine−lutidine hydrohexafluorophosphate, MOPS, PIPES, and BES. The KPF_6/phosphate buffer combination was chosen because in it the Pt-ring background currents were lowest and the kinetic currents for O_2 reduction on a Pt-disk electrode were largest. Although the buffer concentration does not affect the electrochemical behavior in the absence of a substrate, a buffer (>10 mM) is required for catalytic O_2 and H_2O_2 reductions.[55]

A. Cyclic Voltammetry in the Absence of a Substrate. The Fe-only catalysts are stable during multiple CV scans (for at least 2 h) in the absence of a substrate. The $I-E$ profile obtained in the first scan is very similar to those in subsequent scans, and the areas under the curves do not change significantly, suggesting that steady-state behavior is rapidly achieved. There is a gradual loss of charge for the FeCu complexes at reducing potentials (<0 V) indicative of the loss of Cu^I.

B. RRDE Experiments in O_2 Reduction. In pH 7 buffers, the Pt ring was held at 800 mV; although the collection efficiency at larger potentials was somewhat higher, the background current increased significantly. Because of the high overall selectivity of O_2 reduction by our catalysts, it was important to minimize the background currents; the 800 mV ring potential represents the optimum collection efficiency at small background currents. A catalyst-bearing RRDE was immersed in the electrolyte solution, and the Pt ring (polarized at 800 mV) was allowed to equilibrate for 2−4 min while the disk was at an open circuit. After the ring background stabilized, the disk was connected and an LSV was collected.

C. RRDE Experiments with H_2O_2 as Substrate. The Au ring was polarized at −300 mV. The collection efficiency of the Au ring toward O_2 was measured by carrying out H_2O_2 oxidation at the Pt disk of the Au-ring/Pt-disk rotating electrode, factoring out the O_2 flux resulting from Pt-catalyzed H_2O_2 disproportionation. The equilibration of the Au ring in H_2O_2 containing electrolyte was carried out as described for the Pt ring.

D. Koutecky-Levich Data. Limiting currents for Koutecky−Levich plots were collected potentiostatically to eliminate any effect of catalyst decomposition on the kinetic data and to speed data collection. At a desired rotation rate, the film was polarized for 3 s at −150 mV and the electrode was disconnected; the rotation frequency was changed, and the procedure was repeated. The electrode rotation frequency was changed randomly, so as to eliminate any bias introduced by the data collection order. Distortion of data may arise, for example, from progressive catalyst decomposition in the course of data collection. Using random order of data collection, such decomposition of the catalyst is identified by substantial data scatter. A control experiment showed that the currents acquired potentiostatically were identical to those measured by LSVs.

Table 4. Buffers Employed

pH	buffer
2	$HClO_4$
3	$HClO_4$; *o*-$C_6H_4(CO_2H)_2$/$(NH_2)SO_2(OH)$/KOH
4, 4.5	*o*-$C_6H_4(CO_2H)_2$/KOH; NaO_2CCH_3/HO_2CCH_3; citric acid/KOH
6.3, 7, 7.8	Na_2HPO_4/KH_2PO_4; PIPES; MOPS; BES
9	$Na_2CO_3/NaHCO_3$; CHES
10, 10.5	$Na_3PO_4/NaHCO_3$
11	KOH; $Na_3PO_4/NaHCO_3$
12	KOH

E. pH Dependence of $E_{1/2}$. The list of the employed buffers is given in Table 4. At pH values other than 2 and 12, the experiments were conducted in at least two different buffers to eliminate a possibility that the reactivity is attenuated by a particular anion. O_2 concentrations in various pH electrolytes were similar. The pH dependence of $E_{1/2}$ was measured from LSVs at 200 rpm at the catalyst coverage 2.5 nmol/cm^2. Corresponding Tafel plots had similar slopes at all studied pH values. O_2 reduction at pH values between 6.3 and 9 was also examined with catalytic films of 1 nmol/cm^2. No effect of Γ_t was observed.

F. Measurements of Characteristic Current Densities. The current densities of charge and substrate transfer (j_c and j_S, respectively) were estimated as previously described.[50] Background O_2 reduction at EPG modified with a catalytically inactive ZnCu analogue of the FeCu catalyst (Zn substitutes for Fe) was used to measure j_S. Because O_2 reduction on unmodified EPG is relatively slow ($j_k \leq \sim 3.5$ mA/cm^2), the intercepts of the Koutecky−Levich plots were largely independent of the amount of deposited ZnCu at $\Gamma_t < 25$ nmol/cm^2 and increased approximately linearly with Γ_t in the range 25−50 nmol/cm^2. The value of j_S for catalytic films of 2.5 nmol/cm^2 was obtained by extrapolating the latter data. Although O_2 electroreduction is much faster at thoroughly cleaned Au or Pt surfaces, their facile passivation by even submonolayer amounts of organic adsorbants precluded the use of Pt or Au electrodes for j_S determination in present studies.

G. Measurement of the Turnover Numbers in O_2 Reduction at 200 mV. A regular LSV scan (at 200 rpm) was followed by a potentiostatic run (at 200, 1000, or 2000 rpm) in which the disk potential was kept at 200 mV until a desired amount of current had passed corresponding to an ∼15% loss of catalytic selectivity (6−15 min). After the disk was allowed to equilibrate for 15 s at open circuit, a regular LSV run at 200 rpm was repeated. The TNs were calculated according to the formula: $TN = [(C/nF)/A\Gamma_t]/[1 - (i_r/i_{cat})_{initial}/(i_r/i_{cat})_{final}]$, where C is the total amount of charge (C) passed, $A\Gamma_t$ is the total amount of catalyst (mol), and i_r/i_{cat} is the ring-to-disk current ratio in the initial and final LSV scans (assuming that the collection efficiency does not change during the run). The A, F, and n constants were defined previously.[57] The physical sense of the numerator is the average number of O_2 molecules reduced by one molecule of the catalyst. The calculations assume that all of the catalyst retains its catalytic activity toward O_2 reduction; only its selectivity changes (i.e., $A\Gamma_t$ does not change). Ten independent measurements for each catalyst were performed; the aqueous electrolyte was changed after every third measurement to maintain a high collection efficiency. The reported TNs are averaged values. The ring electrode cannot be used if •OH scavengers are present in electrolyte. The rate of the decrease in O_2 reduction current (as a result of gradual degradation of the catalyst) is not affected by the presence of •OH (up to 100 mM).

H. Measurement of the Turnover Numbers in O_2 Reduction at <−100 mV and H_2O_2 Reduction. The TNs were measured at O_2 concentrations of 0.24 and 1.2 mM and at H_2O_2 concentrations of 50 μM, 3 mM, and 5 mM. A set of limiting currents at different electrode rotations was collected as described above and was followed by a potentiostatic run at the desired potential until the current dropped to

~50−25% of the initial value (10−15 min, depending on the rotation rate).[26] The electrode was disconnected and allowed to equilibrate for 15 s, and another set of limiting currents was collected. The TNs were determined from least-squares fits (to eq 1 in the Results section) of the i_{cat} versus t data in the potentiostatic run. In addition, the TNs were estimated from the difference in the intercepts of the KL graphs using the sets of the limiting currents collected before and after the potentiostatic run. The slopes of the two graphs were within 10% of each other, indicating that the decrease of the kinetic currents is caused by a decrease in the activity of the catalytic film and not by changes in the bulk substrate concentration or the apparent redox stoichiometry of the reduction. Therefore, TNs could be estimated according to the formula: $TN = [C/nFA\Gamma_{cat}]/[1 - i_k^{final}/i_k^{initial}]$, where $n = 4$ (O_2 reduction) or 2 (reduction of H_2O_2). The physical sense of the denominator is the amount of the catalyst that became inactive during the reduction of the C/nF moles of the substrate (O_2 or H_2O_2). The TNs determined by these two methods were comparable; the reported TNs are averaged values. The TNs in the presence of •OH scavengers (between 1 and 50 mM) were determined similarly.

Experiments with Antioxidants or Other Additives in Catalytic Films. Only antioxidants that were (a) soluble in dimethoxyethane or methanol (casting solvents); (b) nonelectrochemically active at 300−0 mV; (c) unreactive toward the catalysts, H_2O_2 and O_2; and that (d) did not affect the $i_{cat}-E$ profiles when present in the film in an at least 0.2 molar fraction were used in these studies. Vitamin C does not satisfy criteria a and b, and α-tocopherol does not satisfy criterion d; therefore, these chemicals could not be used. An O_2 reduction on the EPG disk modified with 5 nmol/cm^2 of pure Zn-only or ZnCu complexes, BHT, α-tocopherol (as a structural and functional analogue of modestly water-soluble trolox), 2,3-naphthalenedicarboxylic acid, and ebselen yields $i_{cat}-E$ curves and the i_r/i_{cat} ratios identical to those obtained with an unmodified EPG disk. No currents were detected below −180 mV (vs NHE, which corresponds to the onset of the catalytic reduction wave on an EPGE). These observations indicate that these compounds do not generate ring-reducible species and are inert toward H_2O_2 (produced by the reduction of O_2 on the graphite). The experiments were done with 10% O_2 in N_2 to compensate for larger fluxes of H_2O_2 arising from the lower selectivity of O_2 reduction on an EPGE. Pure films of *N*-(2-mercaptopropionyl)glycine (MPG) are not stable because of its water-solubility. Therefore, a 1:1 mixed film of Zn-only and MPG was used to check that MPG is inert toward O_2 and H_2O_2 under electrocatalytic conditions.

The mixed films were cast from solutions of the catalysts containing an additive in the desired molar fraction. These mixed solutions were prepared immediately prior to casting. The maximum amount of the additive that did not shift the catalytic curve to more reducing potentials was used. Because of the substantial water-solubility of MPG, its leaching from the film into the aqueous electrolyte is possible, so that the molar fraction of this antioxidant in the modified films may be lower than indicated in Table 1. Experiments with FeCu−MPG films are inconclusive because of the possible extraction of Cu by the thiol groups of MPG.

A LSV was performed as with unmodified films. LSVs on unmodified films were collected, followed immediately by collecting LSVs of modified films, to ensure reproducible experimental conditions. At least five experiments (using freshly prepared films each time) for each additive were performed, and the results were averaged.

Acknowledgment. We thank Profs. C. E. D. Chidsey (Stanford) and R. W. Murray (North Carolina) for their invaluable comments. We acknowledge the financial support from NSF, NIH, and a Stanford Graduate Fellowship (R.B.).

Supporting Information Available: Mathematical analysis of the $E_{1/2}$ versus pH dependence and additional electrochemical data. This material is available free of charge via the Internet at http://pubs.acs.org.

JA026179Q